Advances in Applied Mathematics and Mechanics
Adv. Appl. Math. Mech., Vol. **11**, No. 2, pp. 312-337

DOI: 10.4208/aamm.OA-2018-0130
April 2019

A Generalized Local Grid Refinement Approach for Modeling of Multi-Physicochemical Transports by Lattice Boltzmann Method

Amer Alizadeh and Moran Wang*

Department of Engineering Mechanics and CNMM, Tsinghua University, Beijing 100084, China

Received 31 May 2018; Accepted (in revised version) 12 August 2018

Abstract. The multi-physical transport phenomena through the different size geometries are studied by developing a general local grid refinement approach for lattice Boltzmann methods. Revisiting the method of local fine patches on the coarse grid, through the Chapman-Enskog expansion, the multi-physicochemical source terms such as ion electro-migration, heat source, electric body force, and free net electric charge density can be rigorously incorporated to the rescaling relations of the distribution functions, which interchange between fine and coarse grids. We propose two general local refinement approaches for lattice Boltzmann for momentum and advection-diffusion equations with source terms. To evaluate our algorithm, (i) a body-force driven Poiseuille flow in a channel; (ii) an electro-osmotic flow in which the coupled Poisson-Nernst-Planck with Navier-Stokes equations for overlapped and non-overlapped electric double layers; (iii) a symmetric and asymmetric 1D and 2D heat conduction with heat generation in a flat plate; and (iv) an electric potential distribution near a charged surface, are modeled numerically. Good agreements with the available analytical solutions demonstrated the robustness of the proposed algorithm for diffusion or advection-diffusion equations, which may be coupled or decoupled. The present model may broaden the applications of local grid refinement for modeling complex transport phenomena, such as multi-physicochemical transport phenomena in different size geometries.

AMS subject classifications: 65N50, 74S30

Key words: Local grid refinement, lattice Boltzmann model, source term, multiscale geometry, multi-physics.

*Corresponding author.
Email: mrwang@tsinghua.edu.cn (M. R. Wang)

1 Introduction

At recent decade, investigating mechanisms of multi-physicochemical transport phenomena has been of great interests with important applications in micro- and nanosystems [1–7]. To study the transport mechanism, the uniform grid lattice Boltzmann method as an efficient and inexpensive method has been widely used recently [8–12]. However, in real applications, for different size (e.g., micro-nano conjunction) problems or problems with a high gradient of physical properties region, the uniform grids would not retain the major superiority of the lattice Boltzmann method over other computational methods. To deal with this challenge, several attempts have been drawn to improve the adequate grid resolution of the lattice Boltzmann method [13–19]. For this purpose, the local grid refinement method has been proposed based on the concept of the hierarchical grid refinement with higher applicability, accuracy, and efficiency [20].

The first employing of second-order local grid refinement technique for the lattice Boltzmann model was developed by Filippova and Hanel [21], which hereinafter is so called as FH model. In their work, the whole domain is covered by a coarse grid. For regions where large changes of macroscopic properties are expected, fine grids are superposed to the coarse grid. In addition, for the adaptive mesh refinement methods, one can adapt the size and number of superposed fine patches [22]. By considering the same viscosity and, as a result, the same Reynolds number for two grids, the relaxation parameters could be redefined for fine grids. For a pressure driven flow over a circular cylinder, the drag (C_D), lift (C_L) and pressure difference (ΔP) coefficients have good agreements with the available experiments [23]. Later, Filippova and Hanel [20] developed their model in which the molecular velocities in the fine and coarse grids could be different. It should be mentioned that the Reynolds number for both fine and coarse grids is retained identical. Lin and Lai [24] proposed a simpler algorithm without considering the rescaling of distribution functions when transformed from coarse to fine grid and vice versa. However, this assumption may impose some inaccuracy since the non-equilibrium part of the distribution function has been ignored. Dupuis and Chopard [25] showed that how the approximation of the non-equilibrium distribution function without external force could resolve the singularity problem of the FH model when the relaxation parameters were close to 1.0. For the applicability of the local grid refinement technique, Rohde et al. [26] indicated that their methods were capable of accurately describing the experimental data. To extend the applicability of modeling different flow regimes, Lagrava et al. [27] proposed a method to interchange data for fine-coarse grids under high Reynolds number. Moreover, Eitel-Amor et al. [28] proposed a local hierarchical adaptive grid refinement using the cell-centered lattice structure. They demonstrated that the proposed method could be applied for modeling high Reynolds number flow regimes over a sphere or a circular cylinder. Considering other transport phenomena, Liu et al. [29] reported a two-dimensional multi-block lattice Boltzmann model for solute transport in a shallow water based on the advection-diffusion equation without source term. Stiebler et al. [30] extended the advection-diffusion LB scheme for the hierarchical grids based on

the advection-diffusion LB algorithms which proposed by Ginzburg [31]. They proposed that the coupled different resolution grids could be introduced to the advection-diffusion equation by appropriate interpolations in space and time.

Since the lattice Boltzmann method has been employed extensively to model various emerging micro and nano-scale phenomena [32,33], it is crucial to develop the local grid refinement techniques for the multi-physicochemical transport phenomena to save computational costs. For instance, the intersection of the micro- and nanochannel [34,35] or at the interface of nanoporous media and aqueous solution [36] has been exhibited interesting phenomena such as ion concentration polarization. In order to model and understand this phenomenon, employing finer mesh for the nanoscale part of the system is crucial to meet two demands: (I) saving computational costs and (II) acquiring desirable accuracy. However, considering previous efforts demonstrated that, to our best knowledge, no robust and general local grid refinement method has been proposed for the lattice Boltzmann modeling of the multi-physics by considering the presence of heat source, body force, electro-migration, or free net charge density. The aim of this contribution is to develop a general lattice Boltzmann local grid refinement model for coupled or decoupled diffusion and advection-diffusion equations where the effects of the multi-physics transports have been considered. To meet this aim, we develop generalized lattice Boltzmann models for momentum and advection-diffusion equations. In these equations, the relevant source terms are rigorously added to the governing equations in fine and coarse regions. By employing the Chapman-Enskog expansion and neglecting the higher orders of the small value (ε), we could incorporate the source terms to the fine and coarse grids transformation equations. This assumption of neglecting higher orders of the ε is available since in the present contribution we consider low Reynolds fluid flows. Moreover, the equations to transport the data from fine to coarse and vice versa are modified for when the source terms are involved in the governing equations. It is worth pointing out that the method of present work to incorporate the source term to transformation relations of fine-coarse grids could be followed with other proposed local grid refinement methods [24,25,27,37–40]. The paper is organized as follows. In Section 2, we proposed the developed local grid refinement algorithm for momentum and general advection-diffusion equations with source term. In Section 3, a body force-driven Poiseuille flow, a multi-physicochemical transport (an electro-osmotic flow), one-dimensional and two-dimensional heat conduction with heat source, and the electric potential near to a charged wall are investigated, respectively, to examine the robustness and accuracy of our model. After validating the present work local grid refinement algorithm, in order to demonstrate the necessity of using the new local grid refinement algorithm for equations with source term, we study the applicability of the FH model in Section 4.

2 Mathematical and numerical models

2.1 Momentum and lattice Boltzmann evolution equations

For a multi-component constant-property Newtonian fluid flow, the governing equations for laminar flow are [41,42]

$$\frac{\partial \rho}{\partial t}+\nabla\cdot(\rho\mathbf{u})=0, \tag{2.1a}$$

$$\frac{\partial(\rho u)}{\partial t}+\mathbf{u}\cdot\nabla(\rho\mathbf{u})=-\nabla p+\nabla\cdot(\nu\nabla(\rho\mathbf{u}))+F, \tag{2.1b}$$

where ρ (kg/m^3) is the density of the electrolyte, $\mathbf{u}$ (m/s) the flow velocity vector, t (s) the time, p (Pa) the fluid pressure, v (m^2/s) the kinematic viscosity and F (N/m^3) the body force density which may include all the implemented body forces such as electrical field force or pressure gradient.

The general discrete uniform-grid lattice Boltzmann density distribution equation for solving the Navier-Stokes equations in the presence of external forces is indicated as follows [43]

$$f_i(\mathbf{X}+\mathbf{e}_i\delta_t,t+\delta_t)-f_i(\mathbf{X},t)=-\frac{1}{\tau_v}\left[f_i(\mathbf{X},t)-f_i^{eq}(\mathbf{X},t)\right]+\delta_t F_i, \tag{2.2}$$

where index i is assigned values from 0 to 8 in the standard D2Q9 lattice (Fig. 1) and f_i the density distribution function at place $\mathbf{X}$ and time t. The relaxation time τ_v is related to the kinematic viscosity as $\nu=(1/3)(\tau_v-0.5)\delta_t$. F_i is the general format of the external force distribution function at the same time and place and defined as follows [44]

$$F_i=\frac{(-\nabla p+\rho_e(\mathbf{E}-\nabla\psi))\cdot(\mathbf{e}_i-\mathbf{u})}{\rho c^2}f_i^{eq}, \tag{2.3}$$

where the ∇p and $\rho_e(\mathbf{E}-\nabla\psi)$ represent the external pressure gradient and the electrical body force, respectively, while $\mathbf{E}$, and $\nabla\psi$ denote the applied external electric field and

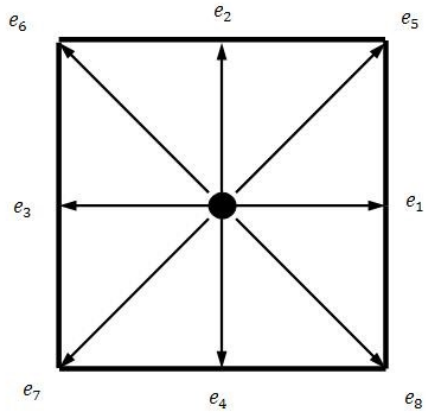

Figure 1: The D2Q9 lattice discrete velocities.

the electric field due to the distribution of the ions. The Maxwell-Boltzmann equilibrium distribution function for Eqs. (2.2) and (2.3) is [45]

$$f_i^{eq}=\omega_i\rho\left[1+\frac{3(\mathbf{e_i}\cdot\mathbf{u})}{c^2}+\frac{9(\mathbf{e}_i\cdot\mathbf{u})^2}{2c^4}-\frac{3}{2}\frac{(\mathbf{u}\cdot\mathbf{u})}{c^2}\right], \tag{2.4}$$

where $\mathbf{u}$ is the macroscopic velocity vector and ρ is the density of the fluid. ω_i represents the weighting factors for D2Q9 lattice as follows:

$$\begin{cases} \omega_i=4/9, & i=0, \\ \omega_i=1/9, & i=1,2,3,4, \\ \omega_i=1/36, & i=5,6,7,8. \end{cases} \tag{2.5}$$

After evolution, the macroscopic values of the density and velocity are calculated as follows:

$$\rho=\sum_{i=0}^{8}f_i, \tag{2.6a}$$

$$\rho u=\sum_{i=0}^{8}f_i e_i. \tag{2.6b}$$

2.1.1 Local grid refinement algorithm for momentum equation with source term

Using the local grid refinement method for the region with large gradients of the physical properties not only reduces the computational time and cost but also causes more stable and accurate results. The strategy of the local grid refinement approach is simple and straightforward [21]. Firstly, whole computational domain is covered by coarse grids. Second, for the regions where high resolution is desired, patches of fine grids will be superposed on the coarse grid. Obviously, the fine grid patch has two types of nodes on the fine-coarse boundary as, (1) the nodes which coincide on the coarse nodes; (2) the nodes place between the coarse nodes which are so-called hanging nodes. Considering the hanging nodes, the distribution functions on the coarse grids should be temporally and spatially interpolated to find out the related coarse distribution functions. Thus, in order to provide higher accuracy, the interpolation procedure is of great importance. In this contribution, we have employed the second-order spatially and temporally Lagrange interpolation. Fig. 2 illustrates the configuration of a coarse grid with a superposed fine grid. From the physical point of view, the macroscopic parameters in a locally refined lattice system should be identical in different grids. Therefore, for fluid flow, the viscosity, velocity, density (as a result the Reynolds number) and body force should be identical in different grids.

Superposing a fine patch grid on a coarse grid will divide the space step through a refinement factor as $m=\frac{\delta_{x,c}}{\delta_{x,f}}$. Considering the general format of the lattice Boltzmann

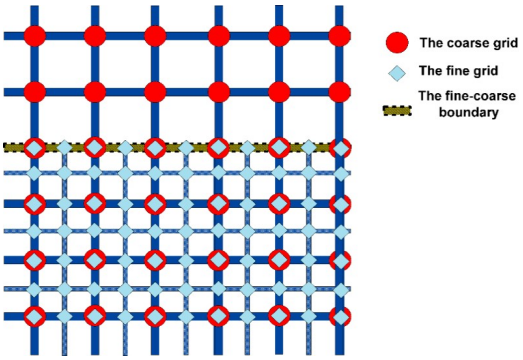

Figure 2: The illustration of a fine-coarse grid configuration. The hanging nodes depicted by the diamonds symbols lying on the fine-coarse boundary.

equation with source term (Eq. (2.2)), one can rewrite it as

$$f_i^{pc}=\left(1-\frac{1}{\tau_v}\right)f_i+\frac{1}{\tau_v}f_i^{eq}+\varepsilon F_i, \tag{2.7}$$

where f_i^{pc} denotes the post-collision distribution function, ε is a very small amount which is attributed to the δ_t. It is noted that F_i could be grid dependent or independent value. However, for a simple body-force driven flow, F_i is defined as [44]

$$\mathbf{F}_i=\frac{(\bar{\mathbf{F}})\cdot(e_i-u)}{\rho c^2}f_i^{eq}, \tag{2.8}$$

where $\overline{\mathbf{F}}$ represents the body force which is exerted to the whole region of the fluid flow. In this work, we assume that both the space and time are divided by the fine grid refinement factor. Consequently, the lattice speed for fine and coarse grids would be identical ($c_c=c_f$). Considering what mentioned above, one can point out that the equilibrium distribution function over local refined lattice systems should be equal ($f_i^{eq,c}=f_i^{eq,f}$) since the velocity, density and lattice speed are identical for different grids (Eq. (2.4)).

Taking a Taylor expansion from the left-hand side of Eq.(2.2) in space and time provides [20]

$$\varepsilon(D_t f_i)+\frac{1}{2}\varepsilon^2\left(D_t^2 f_i\right)+\mathcal{O}\left(\varepsilon^3\right)=-\frac{1}{\tau_v}\left(f_i-f_i^{eq}\right)+\varepsilon F_i, \tag{2.9}$$

where $D_t=\left(\frac{\partial}{\partial t}+e_{ij}\frac{\partial}{\partial x_j}\right)$ denotes the total derivative operator. Here, we point out that based on the assumption of the continuous physical space in the limit of small ε, the source term at right-hand side of Eq. (2.2) could be written as εF_i. Using the first-order

Chapman-Enskog expansion for both fine and coarse distribution functions gives rise to

$$f_i^c = f_i^{eq,c} + \varepsilon_c f_i^{(1),c} + \mathcal{O}\left(\varepsilon_c^2\right), \tag{2.10a}$$

$$f_i^f = f_i^{eq,f} + \varepsilon_f f_i^{(1),f} + \mathcal{O}\left(\varepsilon_f^2\right), \tag{2.10b}$$

where ε_c and ε_f represent the coarse and fine grids small amounts, respectively, which could be noted as $\varepsilon_c = \delta_{(x,c)}$ and $\varepsilon_f = \delta_{(x,f)}$. Substituting Eq. (2.10) into Eq. (2.9) and equating the same order of ε, one has

$$D_t f_i^{(0)} = -\frac{1}{\tau_v} f_i^{(1)} + F_i, \tag{2.11}$$

where $f_i^{(0)} = f_i^{eq}$ and Eq. (2.11) could be written as

$$f_i^{(1)} = \tau_v \left(F_i - D_t f_i^{eq}\right). \tag{2.12}$$

As mentioned above, in a local refinement lattice Boltzmann model, the term $F_i - D_t f_i^{eq}$ should be identical for both fine and coarse grids. We define $\xi = F_i - D_t f_i^{eq}$ as a constant parameter over different grids. Introducing Eq. (2.12) to Eqs. (2.10a) and (2.10b), we have

$$\xi = \frac{f_i^c - f_i^{eq,c}}{\varepsilon_c \tau_v^c} = \frac{f_i^f - f_i^{eq,f}}{\varepsilon_f \tau_v^f}, \tag{2.13}$$

where τ_v^c and τ_v^f represent the relaxation time for coarse and fine grids, respectively. By considering the non-equilibrium definition ($f_i^{neq} = f_i - f_i^{eq}$) for both fine and coarse grids, Eq. (2.13) could give

$$f_i^{neq,c} = m \frac{\tau_v^c}{\tau_v^f} f_i^{neq,f}, \tag{2.14}$$

where $m = \frac{\delta_{x,c}}{\delta_{x,f}} = \frac{\varepsilon_c}{\varepsilon_f}$. Rewriting Eq. (2.7) in the form of non-equilibrium for coarse grid

$$f_i^{pc,c} = f_i^{eq,c} + \left(\frac{\tau_v^c - 1}{\tau_v^c}\right) f_i^{neq,c} + \varepsilon_c F_i^c \tag{2.15}$$

and substituting Eq. (2.14) into it, by considering the equality of the equilibrium distribution functions for different grids, we have

$$f_i^{pc,c} = f_i^{eq,f} + m \frac{\tau_v^c - 1}{\tau_v^f} f_i^{neq,f} + \varepsilon_c F_i^c. \tag{2.16}$$

The $f_i^{neq,f}$ in Eq. (2.16) could be substitute as

$$f_i^{neq,f} = \left(\frac{\tau_v^f}{\tau_v^f - 1}\right)\left(f_i^{pc,f} - f_i^{eq,f} - \varepsilon_f F_i^f\right). \tag{2.17}$$

By introducing Eq. (2.17) into Eq. (2.16), finally, the relation for transforming data from fine to coarse grid for momentum equations with source term is developed as

$$f_i^{pc,c} = f_i^{eq,f} + m\left(\frac{\tau_v^c - 1}{\tau_v^f - 1}\right)\left(f_i^{pc,f} - f_i^{eq,f} - \varepsilon_f F_i^f\right) + \varepsilon_c F_i^c. \tag{2.18}$$

Eq. (2.18) proposes the rescaling relation when distribution functions are transforming from fine to coarse grid. It is worth noting that two added terms, $\varepsilon_f F_i^f$ and $\varepsilon_c F_i^c$, represent the source term of Eq. (2.9) in rescaling relations. However, still the transmitted distribution functions should be rescaled when transform from coarse to fine grid. To this purpose, in a similar approach to what was performed for Eq. (2.18), the distribution functions transformed from coarse to fine grids could be rescaled as

$$f_i^{pc,f} = \tilde{f}_i^{eq,c} + \frac{1}{m}\left(\frac{\tau_v^f - 1}{\tau_v^c - 1}\right)\left(\tilde{f}_i^{pc,c} - \tilde{f}_i^{eq,c} - \varepsilon_c F_i^c\right) + \varepsilon_f F_i^f, \tag{2.19}$$

where $\varepsilon_c = \delta_{t,c}$, $\varepsilon_f = \delta_{t,f}$ and $\tilde{f}_i$ define the spatially and temporally interpolated values of the distribution functions from coarse grids on the fine-coarse boundary. As mentioned before, since the viscosity and as a result the Reynolds number should be same in a local refined lattice system, by considering the definition for viscosity as $\nu = \frac{(2\tau-1)\delta_x c}{6}$, one can find out the relaxation parameter for the fine grids as [21]

$$\omega_f = \frac{2}{1 + m\left(\frac{2}{\omega_c} - 1\right)}, \tag{2.20}$$

where ω denotes the relaxation parameter as $\omega = 1/\tau$.

Here we should note that the proposed local grid-refinement method provides second-order accuracy in space for when the Mach number of the flow would be on the order of Knudsen number.

2.2 General advection-diffusion and lattice Boltzmann evolution equations with source term

The conservation equation which governs the transport phenomena and includes the advection-diffusion with a source term could be generally written as

$$\frac{\partial \phi(\mathbf{X},t)}{\partial t} + u \cdot \nabla \phi(\mathbf{X},t) = D_\phi \nabla^2 \phi(\mathbf{X},t) + \varphi(\mathbf{X},t), \tag{2.21}$$

where $\phi(\mathbf{X},t)$, D_ϕ, and $\varphi(\mathbf{X},t)$ represent the property distribution in time and space, the diffusion coefficient of the property, and the source term which may affect the distribution of the property spatially and temporally, respectively. On the other hand, considering the lattice Boltzmann evolution equation for different advection-diffusion phenomena including source terms, a general format for lattice Boltzmann evolution equation

can be presented as

$$\Phi_i(\mathbf{X}+e_i\delta_{t,\Phi},t+\delta_{t,\Phi})-\Phi_i(\mathbf{X},t)=-\frac{1}{\tau_\Phi}\left[\Phi_i(\mathbf{X},t)-\Phi_i^{eq}(\mathbf{X},t)\right]+\delta_{t,\Phi}F_{\varphi,i}, \tag{2.22}$$

where Φ_i, Φ_i^{eq}, τ_Φ, and $\delta_{(t,\Phi)}$ represent the distribution function, equilibrium distribution function, relaxation time which is defined as $\tau_\Phi=(3D_\phi)/(2c_\phi\delta_x)+0.5$, and time step for a specified transport phenomenon (i.e., heat, ion or electric potential), respectively. In Eq. (2.22), the lattice speed of transferring date is defined as $c_\phi=\delta_x/\delta_t$. It should be pointed out that $F_(\varphi,i)$ represents the specific lattice Boltzmann source term and generally defined as [46]

$$\mathbf{F}_{\varphi,i}=\omega_i\left(1-\frac{0.5}{\tau_\Phi}\right)\varphi(\mathbf{X},t), \tag{2.23}$$

where $\varphi(\mathbf{X},t)$ is the source term which is denoted in Eq. (2.21). Obviously, the term $\varphi(\mathbf{X},t)$ should be an independent term of the grid size in our local refined lattice system. It is worth pointing out that there is another format of forcing term which is more accurate and complex [47] than the conventional forcing term (Eq. (2.24)). The weighting factor, ω_i, would be similar as those defined in Eq. (2.5). The general Maxwell-Boltzmann equilibrium distribution function for Eq. (2.22) is

$$\Phi_i^{eq}=-\bar{\vartheta}_i\phi(\mathbf{X},t)\frac{3\mathbf{u}\cdot\mathbf{u}}{2C^2}, \qquad i=0, \tag{2.24a}$$

$$\Phi_i^{eq}=\bar{\vartheta}_i\phi(\mathbf{X},t)\left[\frac{3}{2}+\frac{3\mathbf{e}_i\cdot\mathbf{u}}{2c^2}+\frac{9(\mathbf{e}_i\cdot\mathbf{u})^2}{2c^2}-\frac{3\mathbf{u}\cdot\mathbf{u}}{2c^2}\right], \qquad i=1,2,3,4, \tag{2.24b}$$

$$\Phi_i^{eq}=\bar{\vartheta}_i\phi(\mathbf{X},t)\left[3+\frac{6\mathbf{e}_i\cdot\mathbf{u}}{c^2}+\frac{9(\mathbf{e}_i\cdot\mathbf{u})^2}{2c^2}-\frac{3\mathbf{u}\cdot\mathbf{u}}{2c^2}\right], \qquad i=5,6,7,8, \tag{2.24c}$$

where $\bar{\vartheta}_i$ is the equilibrium weighting factors and defined as the same as ω_i,

$$\bar{\vartheta}_i=\begin{cases}\dfrac{4}{9}, & i=0,\\ \dfrac{1}{9}, & i=1,2,3,4,\\ \dfrac{1}{36}, & i=5,6,7,8.\end{cases} \tag{2.25}$$

Finally, the macroscopic amounts of the properties are obtained as

$$\phi(\mathbf{X},t)=\left(\sum_{i=0}^{8}\Phi_i+\frac{\delta_{t,\Phi}}{2}F_{\varphi,i}\right). \tag{2.26}$$

2.2.1 Local grid refinement method for advection-diffusion equations with source term

The same approach with Section 2.1 is employed to obtain the rescaling relations for distribution functions in a general advection-diffusion equation with source term. By introducing the Chapman-Enskog expansion

$$\Phi_i^c = \Phi_i^{eq,c} + \varepsilon_c \Phi_i^{(1),c} + \mathcal{O}\left(\varepsilon_c^2\right), \tag{2.27a}$$

$$\Phi_i^f = \Phi_i^{eq,f} + \varepsilon_f \Phi_i^{(1),f} + \mathcal{O}\left(\varepsilon_f^2\right), \tag{2.27b}$$

to Eq. (2.22) and considering the same order of ε, one has

$$\Phi_i^{(1)} = \tau_\Phi \left(F_{\varphi,i} - D_t \Phi_i^{eq}\right). \tag{2.28}$$

Substituting Eq. (2.24) into Eq. (2.28), we have

$$\Phi_i^{(1)} = \tau_\Phi \left(\left(1 - \frac{0.5}{\tau_\Phi}\right) \omega_i \varphi(\mathbf{X},t) - D_t \Phi_i^{eq} \right). \tag{2.29}$$

Eq. (2.29) shows that the source term could be divided into two terms as the grid dependent term $(1-0.5/\tau_\Phi)$ and the grid independent term which is represented by $\omega_i\varphi(\mathbf{X},t)$. In order to make a grid independent parameter, Eq. (2.29) could be written as

$$\Phi_i^{(1)} = \tau_\Phi \left(\omega_i \varphi(\mathbf{X},t) - D_t \Phi_i^{eq}\right) - 0.5\omega_i \varphi(\mathbf{X},t). \tag{2.30}$$

So, we define $\xi = \omega_i\varphi(\mathbf{X},t) - D_t\Phi_i^{eq}$ as a grid independent parameter. If Eq. (2.30) introduces to Eqs. (2.27a) and (2.27b), we have

$$\xi = \frac{\Phi_i^c - \Phi_i^{eq,c} + \frac{\varepsilon_c \omega_i \varphi(\mathbf{X},t)}{2}}{\varepsilon_c \tau_\Phi^c} = \frac{\Phi_i^f - \Phi_i^{eq,f} + \frac{\varepsilon_f \omega_i \varphi(\mathbf{X},t)}{2}}{\varepsilon_f \tau_\Phi^f}. \tag{2.31}$$

By taking into account the non-equilibrium distribution function definition, Eq. (2.31) gives rise to

$$\Phi_i^{neq,c} = \frac{\varepsilon_c \tau_\Phi^c}{\varepsilon_f \tau_\Phi^f} \Phi_i^{neq,f} + \varepsilon_c \left(\frac{\tau_\Phi^c}{\tau_\Phi^f} - 1\right) \left(\frac{\omega_i \varphi(\mathbf{X},t)}{2}\right). \tag{2.32}$$

Rewriting Eq. (2.22) in a non-equilibrium format (similar to Eq. (2.15)) and substituting Eq. (2.32) in it, one has

$$\Phi_i^{pc,c} = \Phi_i^{eq,c} + m \frac{\tau_\Phi^c - 1}{\tau_\Phi^f} \Phi_i^{neq,f} + \frac{\varepsilon_c}{2} \left(\frac{\tau_\Phi^c - 1}{\tau_\Phi^f} + 1\right) \omega_i \varphi(\mathbf{X},t). \tag{2.33}$$

Moreover, by rewriting Eq. (2.22) in the non-equilibrium format for fine grid, one could find out the fine non-equilibrium term as

$$\Phi_i^{neq,f}=\left(\frac{\tau_\Phi^f}{\tau_\Phi^f-1}\right)\left(\Phi_i^{pc,f}-\Phi_i^{eq,f}-\varepsilon_f\left(1-\frac{0.5}{\tau_\Phi^f}\right)\omega_i\varphi(\mathbf{X},t)\right). \tag{2.34}$$

Finally, the rescaling relation for distribution functions transforming from fine to coarse grids could be obtained when Eq. (2.34) substitutes into Eq. (2.33) as

$$\begin{aligned}\Phi_i^{pc,c}=&\Phi_i^{eq,f}+m\frac{\tau_\Phi^c-1}{\tau_\Phi^f-1}\left(\Phi_i^{pc,f}-\Phi_i^{eq,f}-\varepsilon_f\left(1-\frac{0.5}{\tau_\Phi^f}\right)\omega_i\varphi(\mathbf{X},t)\right)\\&+\frac{\varepsilon_c}{2}\left(\frac{\tau_\Phi^c-1}{\tau_\Phi^f}+1\right)\omega_i\varphi(\mathbf{X},t).\end{aligned} \tag{2.35}$$

With a similar approach for Eq. (2.35), the rescaling relation for distribution function transforming from coarse to fine grid is obtained as

$$\begin{aligned}\Phi_i^{pc,f}=&\tilde{\Phi}_i^{eq,c}+\frac{1}{m}\frac{\tau_\Phi^f-1}{\tau_\Phi^c-1}\left(\tilde{\Phi}_i^{c}-\tilde{\Phi}_i^{eq,c}-\varepsilon_c\left(1-\frac{0.5}{\tau_\Phi^c}\right)\omega_i\varphi(\mathbf{X},t)\right)\\&+\frac{\varepsilon_f}{2}\left(\frac{\tau_\Phi^f-1}{\tau_\Phi^c}+1\right)\omega_i\varphi(\mathbf{X},t),\end{aligned} \tag{2.36}$$

where $\tilde{\Phi}_i$ denotes the spatially and temporally interpolated coarse grid distribution functions on the hanging nodes. Since the diffusion coefficient in a local refined lattice system should be identical for different grids, by considering the general definition of the relaxation time as $\tau_\Phi=\frac{3D_\phi}{2c_\phi\delta_x}+0.5$, it is found that the relation between relaxation parameter of fine and coarse grid would be the same as what defined by Eq. (2.20). So, we have

$$\omega_{f,\Phi}=\frac{2}{1+m\left(\frac{2}{\omega_{c,\Phi}}-1\right)}. \tag{2.37}$$

3 Benchmarks

3.1 Body-force driven Poiseuille flow

In order to validate our local grid refinement lattice Boltzmann model for momentum equations with the presence of a source term (Section 2.1), we have solved a simple body-force driven Poiseuille flow in a channel. To this aim, a 1D microchannel which the fluid flow is driven by a uniform body force has been considered. By solving Eq. (2.1) with

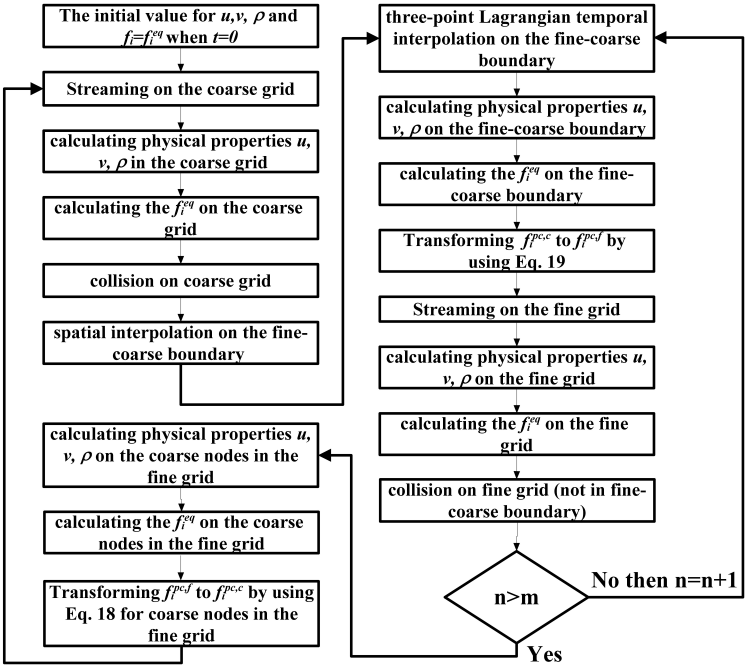

Figure 3: The numerical approach for solving the momentum equations in the present work local grid refinement lattice Boltzmann model.

proper boundary conditions (non-slip velocity boundary conditions at the wall), one has the analytical solution for velocity as

$$U(y)=\frac{H^2}{\bar{U}}\left(\frac{\bar{F}_x}{2\mu}\right)\left(\frac{y}{H}-\left(\frac{y}{H}\right)^2\right), \tag{3.1}$$

where, μ is the dynamic viscosity (Pa$\times$s), H the width of the channel, and $\bar{F}_x$ the component of the body force in the channel length direction. The problem is subjected to a steady-state at $Re=80$ and the domain is covered by coarse grids meshed 201×51.

The numerical approach for solving the momentum equations in this section is depicted in Fig. 3.

It should be noted that: (1) transformation of distribution functions from coarse to fine grids (by Eq. (2.19)) must be exclusively performed on the fine-coarse boundary; (2) the fine grid data would be transformed to coarse grid (by Eq. (2.18)) solely on the coarse grids which excluding nodes on the fine-coarse boundaries.

3.1.1 Fine grid patch location effects

It would be of great importance to prove that the proposed local grid refinement algorithm is generally applicable for different location of the fine patch in coarse grid. One common application of this capability could be found in modeling a moving particle in

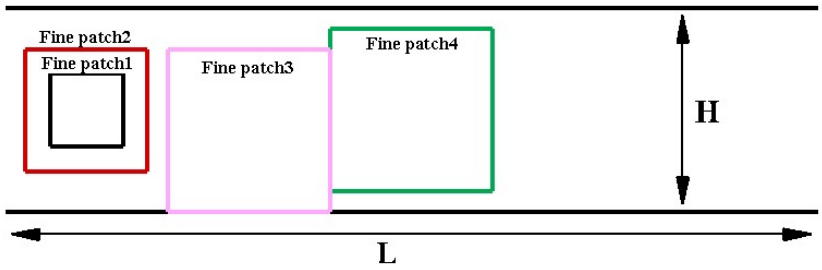

Figure 4: The configuration of the fine grid patches superposed on the coarse grid. The centers of the fine grid patch 1 and 2 are placed in same location with different sizes. Fine patch 3 is positioned with a contact line with the microchannel wall to investigate the ability of the proposed local grid refinement in contact with the boundaries of the main domain.

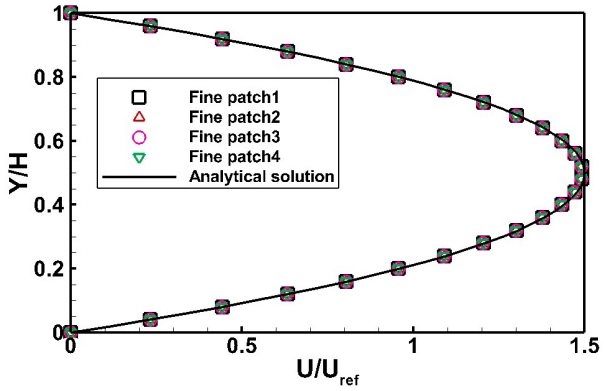

Figure 5: The dimensionless body-force driven Poiseuille velocity along the height of the channel for four fine grid patches compared with the analytical solution.

a fluid. To this purpose, five different fine grid patches with different sizes and locations have been considered in which one patch is located adjacent to the channel wall to examine if the algorithm is applicable near to the coarse grid boundaries (Fig. 4). It should be noted that the refinement factor of the fine grid patches is selected as $m=4$. Fig. 5 illustrates that the presented model predicts dimensionless body-force driven Poiseuille velocities for five patches in a good agreement with the analytical solution.

3.2 Steady-state diffusion transport phenomena

3.2.1 1D and 2D heat conduction with heat generation

In this section, our model is examined for the steady-state diffusion transport phenomena with source term. To this purpose, we employ the general advection-diffusion equation to introduce the local grid refinement algorithm for the heat conduction with heat gen-

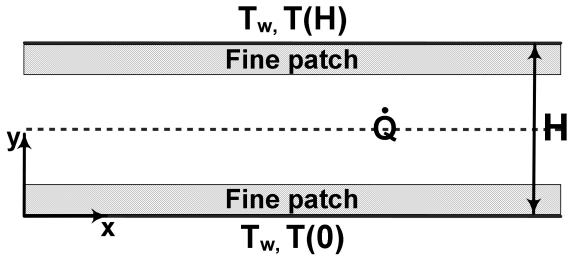

Figure 6: The schematic of a 1D heat conduction with heat generation ($\dot{Q}$) under symmetric ($T(0)=T(H)$) and asymmetric ($T(0)\neq T(H)$) walls temperature.

eration. Generally, the governing equation of the steady-state heat conduction with heat source is [32]

$$\alpha\nabla^2 T=-\left(\frac{1}{\rho c_p}\right)\dot{Q}, \tag{3.2}$$

where α, c_p and $\dot{Q}$ denote the thermal diffusivity coefficient, specific heat capacity and heat generation per unit volume, respectively. Thus, if we set $D_\phi=\alpha$, $\phi(\mathbf{X},t)=T(\mathbf{X},t)$, $\varphi(\mathbf{X},t)=\left(\frac{1}{\rho c_p}\right)\dot{Q}$ and $\mathbf{u}(\mathbf{X},t)=0$ the set of Eqs. (2.21)-(2.26) and Eq. (2.35) and (2.36) will be introduced as the local grid refinement lattice Boltzmann model for heat conduction with source term.

By subjecting a long and narrow plate with heat generation to a symmetric ($T(0)=T(H)=T_w$) and asymmetric ($T(0)=T_w$ and $T(H)=10T_w$ and $50T_w$) uniform wall temperature (Fig. 6), simple analytical solutions for steady-state dimensionless temperature distributions could be obtained as [48]:

$$symmetric:\quad T^*(y)=\frac{T(y)-T_w}{\frac{\dot{Q}H^2}{2K}}=\left(\frac{y}{H}-\left(\frac{y}{H}\right)^2\right), \tag{3.3a}$$

$$asymmetric:\quad T^*(y)=\frac{T(y)-T(0)}{\frac{\dot{Q}H^2}{2K}}=\left(\frac{y}{H}-\left(\frac{y}{H}\right)^2\right)+\frac{T(H)-T(0)}{\frac{\dot{Q}H^2}{2K}}\left(\frac{y}{H}\right), \tag{3.3b}$$

where K in (W/mK) denotes the thermal conductivity of the plate which is uniform in whole problem domain. Fig. 7 shows the perfect agreement of the present work modeling results with analytical solutions (Eq. (3.3a) for 1D symmetric and asymmetric (Eq. (3.3b)) temperature distribution in a narrow plate with heat generation.

In order to examine present work local grid refinement algorithm for 2D heat conduction with a heat source, we consider a 2D flat plate with uniform wall temperatures, thermal conductivity, and heat generation. Fig. 8 shows the schematic of the problem under consideration.

The two fine grid patches were located similarly to what performed for the 1D scenario. For a steady-state 2D heat conduction with heat generation (Eq. (3.2), there would

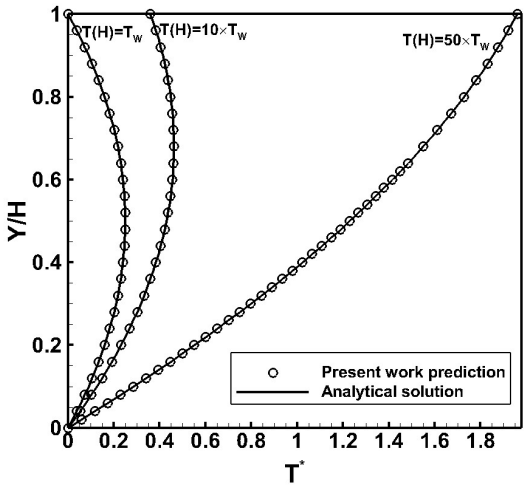

Figure 7: The present work local grid refinement predictions of dimensionless 1D symmetric and asymmetric temperature distribution along the height of a narrow plate with heat generation. The upper wall temperatures are equal to $T(H)=T_w$, $10T_w$, and $50T_w$.

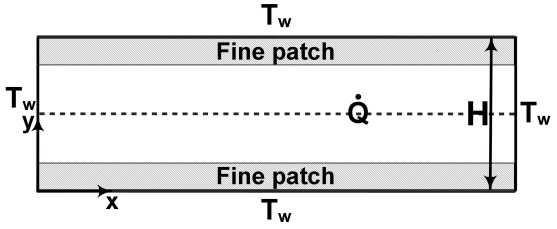

Figure 8: The schematic of a 2D plate subjected to a heat source ($\dot{Q}$) with constant wall temperatures.

be an analytical solution as [48]:

$$T^*(x,y) = \left(1-\left(\frac{x-0.5L}{0.5L}\right)^2\right) - 4\sum_{n=0}^{\infty}\frac{(-1)^n}{(0.5\lambda_n L)^3}\left(\frac{\cosh(\lambda_n(y-0.5H))}{\cosh(0.5\lambda_n H)}\right)\cos(\lambda_n(x-0.5L)), \quad (3.4)$$

where $\lambda_n=\frac{(2n+1)\pi}{L}$ and $n=0,1,2,\cdots$.

Fig. 9 shows that the present work local refinement algorithm also could predict well agreement dimensionless temperature (T^*) with analytical solution.

3.2.2 Electric potential distribution (Poisson-Boltzmann equation)

Although in the last section, we examined the proposed local grid refinement algorithm for a diffusion equation with a uniform source term, however, the applicability of the proposed method should be investigated when the source term would be non-uniformly

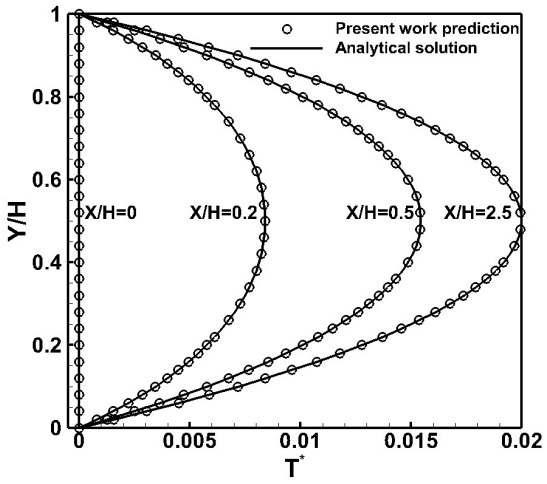

Figure 9: The present work local grid refinement predictions of T^* for a 2D heat conduction with heat generation.

distributed and also depend on the diffused property. Thus, in addition to the energy equation, in this section, the present work model will be examined via a Poisson equation with variable source term. To meet the desired kind of diffusion problem, the distribution of electric potential near a charged surface which is in contact with a binary electrolyte solution is investigated. The governing equation for this problem is [49]

$$\nabla^2\psi=-\frac{\rho_e}{\varepsilon_r\varepsilon_0}=-\left(\frac{1}{\varepsilon_r\varepsilon_0}\right)\left(\sum_{i=1}^{2}ez_in_0\exp\left(-\frac{eZ_i}{k_BT}\psi\right)\right), \tag{3.5}$$

where ρ_e is the net electric charge density which could be obtained by employing the ion Boltzmann distribution equation. The right-hand side of Eq. (3.5) represents a source term which is due to the presence of the free net electric charge density. In Eq. (3.5), ε_r, ε_0, k_B, and z_i, represent the relative electrical permittivity of solution to vacuum, the vacuum electrical permittivity (in C/Vm), the Boltzmann constant number, and the valance number of the ith ion, respectively. Fig. 10 demonstrates the capability of our model to provide good agreements with analytical solutions for three different amounts of $n_0=6.02\times10^{19}$, 1.5×10^{20}, and 5.27×10^{20}(ion/m^3). It is worth pointing out that the analytical solution for Eq. (3.5) would be presented in next section (Eq. (3.13a) in which $\zeta=\psi(X,0)$).

3.3 Multi-physicochemical transport phenomena (coupled Poisson-Nernst-Planck with Navier-Stokes equations)

In many applications, we need to solve the set of coupled equations to model several coupled transport phenomena. For instance, the electro-osmotic flow which is generated due to the motion of the ions near to a charged wall by an applied external electric field is

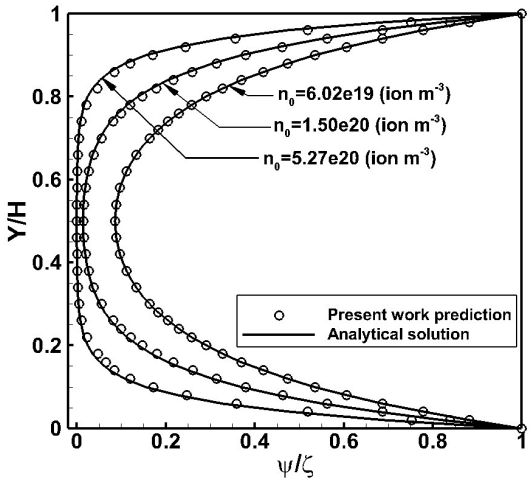

Figure 10: The dimensionless electric potential for the present work local grid refinement lattice Boltzmann model and analytical solution.

a result of three coupled transport phenomena such as (1) the ion transport, (2) the fluid flow, and (3) the internal electric potential [50]. Regarding the governing equation of the ion transport, the mass conservation equation for ith ion species in an electrolyte could be written in general form as [8,51]

$$\frac{\partial C_i}{\partial t}+\nabla\cdot J_i=0, \tag{3.6}$$

where C_i demonstrates the ith ionic concentration, $\mathbf{J}_i$ the species flux. The flux of ith ion, $\mathbf{J}_i$ consisting of electro-migration, diffusion, and advection terms in which by neglecting the dispersion, one has [8]

$$\mathbf{J}_i=-\left(\frac{eZ_iD_i}{KT}\right)C_i\nabla\psi-D_i(\nabla C_i)+C_i\mathbf{u}, \tag{3.7}$$

where the first term on the right-hand side denotes the electrochemical migration, the second term the ions diffusion and the last term the advective transport. In the ions flux equation, e, Z_i, D_i, K and T denote the absolute charge of electron, valance number for ith ion, diffusion coefficient for ith ion, Boltzmann constant, and the absolute temperature, respectively. Introducing Eq. (3.7) into Eq. (3.6), one has

$$\frac{\partial C_i}{\partial t}+\mathbf{u}\cdot\nabla C_i=D_i\nabla^2C_i+\frac{eZ_iD_i}{KT}\nabla\cdot(C_i\nabla\psi). \tag{3.8}$$

The local internal electric potential field, ψ, which is caused by the ion distribution, is governed by the Poisson's equation as mentioned by Eq. (3.5).

Physically, by applying the external electric field, for non-zero net electric charge density, the fluid flow is generated due to the non-zero net moving of the co and counter-ions. The governing equations for fluid flow would be similar to what mentioned in Section 2.1. However, the body force is defined based on the presence of the electrical field as

$$F_i = \frac{\rho_e(\mathbf{E}-\nabla\psi)\cdot(\mathbf{e}_i-\mathbf{u})}{\rho c^2} f_i^{eq}. \tag{3.9}$$

The aims of this section are (1) introducing the coupled local grid refinement algorithms for the Nernst-Planck (ion transport) and the Poisson (electric potential) equations based on the general advection-diffusion local grid refinement algorithm (Section 2.2); and (2) solving the coupled presented lattice Boltzmann models for Poisson, Nernst-Planck, and Navier-Stokes equations numerically in an iteration procedure. It should be noted that the local grid refinement method for the fluid flow is similar to that presented in Section 2.1.

3.3.1 Local grid refinement lattice Boltzmann models for ion transport and electric potential

Based on the general definition for the advection-diffusion equations with source term (Section 2.2), one can simply propose the local grid refinement algorithm for:

1. ion transport as: if we set $D_\phi = D_i$, $\phi(\mathbf{X},t) = C_i(\mathbf{X},t)$, where C_i denotes the local concentration of the ions, and $\varphi(\mathbf{X},t) = \frac{eZ_iD_i}{K_BT}\nabla\cdot(C_i(\mathbf{X},t)\nabla\psi(\mathbf{X},t))$, the set of Eq. (2.21)-(2.26) and Eqs. (2.35) and (2.36) will be introduced as the local grid refinement lattice Boltzmann model for ion transport.

2. electric potential as: if we set $D_\phi = 1$, $(\partial\phi(\mathbf{X},t))/\partial t = 0.0$, $\phi(\mathbf{X},t) = \psi(X,t)$, $\varphi(\mathbf{X},t) = \frac{\rho_e(\mathbf{X},t)}{\varepsilon_r\varepsilon_0}$, and $\mathbf{u}(\mathbf{X},t) = 0$, the set of Eqs. (2.21)-(2.26) and Eqs. (2.35) and (2.36) will be introduced as the local grid refinement lattice Boltzmann model for electric potential.

3.3.2 Problem definition

A straight microchannel with height $H = 6.0(\mu\text{m})$ is considered with uniformly charged walls. The zeta potential on the wall is $\zeta = -25(\text{mV})$ and there would not be any applied pressure gradient. It is assumed that since the electrolyte would be chemically and thermodynamically at equilibrium state, as a result, the well-known ion Boltzmann distribution equation is available and the solution is kept iso-thermal and equal to $T = 293.15(\text{K})$. The electrochemical properties of the solution is selected that the diffusion coefficients of the ions and kinetic viscosity would be constant everywhere in the solution which is $D_{K^+} = D_{Cl^-} = 1.0\times10^{-8}(\text{m}^2/\text{s})$ and $\nu = 8.89\times10^{-7}(\text{m}^2/\text{s})$, respectively. The vacuum electrical permittivity and the ratio of the electrolyte solution permittivity to vacuum permittivity would be $\varepsilon_0 = 8.854\times10^{-12}(\text{C/Vm})$ and $\varepsilon_r = 78.54$, respectively. Electrostatically, the positive ions will attract to the walls and the negative ions repel. As a result, an electric

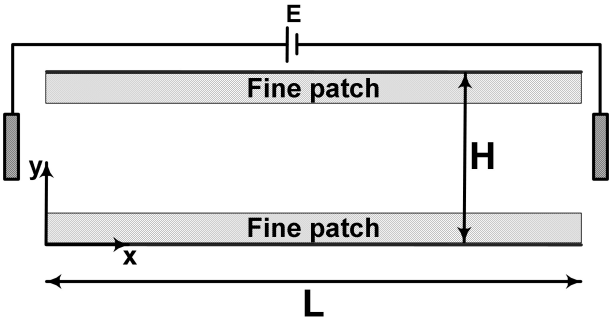

Figure 11: The illustration of fine patches were superposed near to the walls of the microchannel. The walls of the microchannel were negatively charged where the electro-osmotic flow would be generated when an external electric field is applied.

double layer (EDL) is formed near to the charged channel walls. The thickness of the double layer is characterized by the famous Debye length. So, the characteristic electric double layer thickness for the simple binary electrolyte is calculated as

$$\lambda=\kappa^{-1}=\sqrt{\frac{\varepsilon_0\varepsilon_r K_B T}{2Z^2e^2n_0}},$$

where the physical parameters are; electron charge $e=1.602\times10^{-19}$(C), the Boltzmann constant $K_B=1.381\times10^{-23}$(j/K), and the ionic number density n_0, respectively. It is well-realized that the electric double layer has the key role in the electrokinetic transport phenomena [52–54]. Therefore, we superposed two fine grid patches adjacent to the microchannel walls and consider two different dimensionless electrical double layer thicknesses by $n_0=6.022\times10^{19}$ and 1.271×10^{21}(ion/m^3) for $\kappa H=6.29$ and $\kappa H=30.0$, respectively, to verify our model for overlapped and non-overlapped EDLs. Moreover, it is worth noting that the fine grid patches are connected to the walls, inlet, and outlet of the channel to examine our local grid refinement algorithm when superposed on the boundaries of the coarse grid. Fig. 11 illustrates the setup of the electro-osmotic flow and configuration of the coarse and fine grids.

The governing equations in this problem are subjected to the boundary conditions as follows.

Boundary conditions for Navier-Stokes equations are

$$y=0\rightarrow u=v=0,\quad y=H\rightarrow u=v=0, \tag{3.10a}$$

$$x=0\rightarrow\frac{\partial u}{\partial x}=\frac{\partial v}{\partial x}=0,\quad p=P_{atm}, \tag{3.10b}$$

$$x=L\rightarrow\frac{\partial u}{\partial x}=\frac{\partial v}{\partial x}=0,\quad p=P_{atm}. \tag{3.10c}$$

Boundary conditions for the Nernst-Planck equation are

$$y=0 \quad \text{and} \quad y=H \rightarrow C_i=n_0 \exp\left(-\frac{Z_i e\psi}{K_B T}\right), \tag{3.11a}$$

$$x=0 \rightarrow C_i=n_0, \tag{3.11b}$$

$$x=L \rightarrow \frac{\partial C_i}{\partial x}=0. \tag{3.11c}$$

Boundary conditions for Poisson equation are

$$y=0 \quad \text{and} \quad y=H \rightarrow \psi=\zeta_{wall}, \tag{3.12a}$$

$$x=0 \rightarrow \psi=0, \tag{3.12b}$$

$$x=L \rightarrow \frac{\partial \psi}{\partial x}=0. \tag{3.12c}$$

Employing the boundary conditions, the aforementioned multi-physicochemical (ion, electric potential, and fluid flow) local grid refinement algorithms could be solved in coupled iteration procedures (Fig. 12).

For each equation, a similar numerical approach with what was performed for the body-force driven Poiseuille flow has been employed (Fig. 3). However, regarding the distribution functions transformation relations (fine to coarse and vice versa), one has to employ the related relations which we proposed in previous sections. For a solution in a chemically and thermodynamically equilibrium state, the analytical solutions for the electric potential, electro-osmotic velocity, and ion distribution are as [52]:

$$\frac{\psi(y)}{\zeta}=\frac{\cosh\left(\kappa y-\frac{\kappa H}{2}\right)}{\cosh\left(\frac{\kappa H}{2}\right)}, \tag{3.13a}$$

$$\left[1-\frac{u(y)}{U_{ref}}\right]=\frac{\cosh\left(\kappa y-\frac{\kappa H}{2}\right)}{\cosh\left(\frac{\kappa H}{2}\right)}, \tag{3.13b}$$

$$C_i(y)=n_0 \exp\left(-\frac{Z_i e}{K_B T}\psi(y)\right), \tag{3.13c}$$

where U_{ref} represents the Helmholtz-Smoluchowski velocity which is defined as $U_{ref}=\frac{-\zeta\varepsilon_r\varepsilon_0 E_p}{\mu}$ in which the E_p denotes the applied external electric field strength (V/m). Fig. 13 shows the macroscopic properties of electro-osmotic flow with $\kappa H=6.29$, and 30.0 predicted by the coupled local grid refinement lattice Boltzmann models. It is demonstrated that our local grid refinement algorithm could predict good agreements with the analytical solutions for both overlapped ($\kappa H=6.29$) and non-overlapped ($\kappa H=30.0$) electrical double layers.

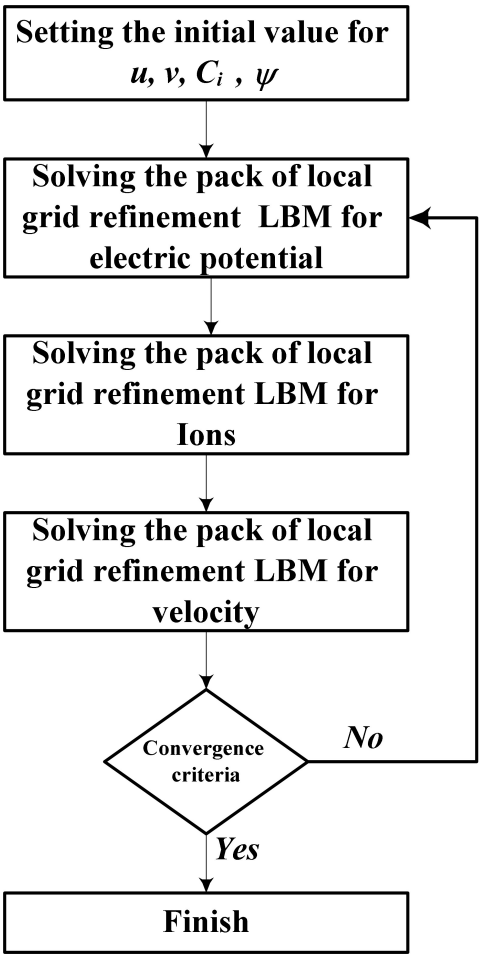

Figure 12: The flowchart diagram of numerical approach for solving the coupled electro-osmotic governing equations. The pack of local grid refinement LBM means the numerical approach which we illustrated at Fig. 3.

4 The applicability of the FH model

In last sections, we have demonstrated that the proposed local grid refinement model predicts well agreement results with available analytical solutions for several different coupled and uncoupled transport phenomena with dependent or independent source terms of diffused property. However, in order to show the necessity of using the proposed model for equations with source term, in this section, we conduct a study on the applicability of the FH model for multi-physics equations with source terms. To this purpose, the Nernst-Planck equation coupled with the Poissons equation are solved based on the FH model for the microchannel defined at Section 3.2.2. Since the source term does not incorporated in the FH model, as a result, the fine-coarse grids transformation

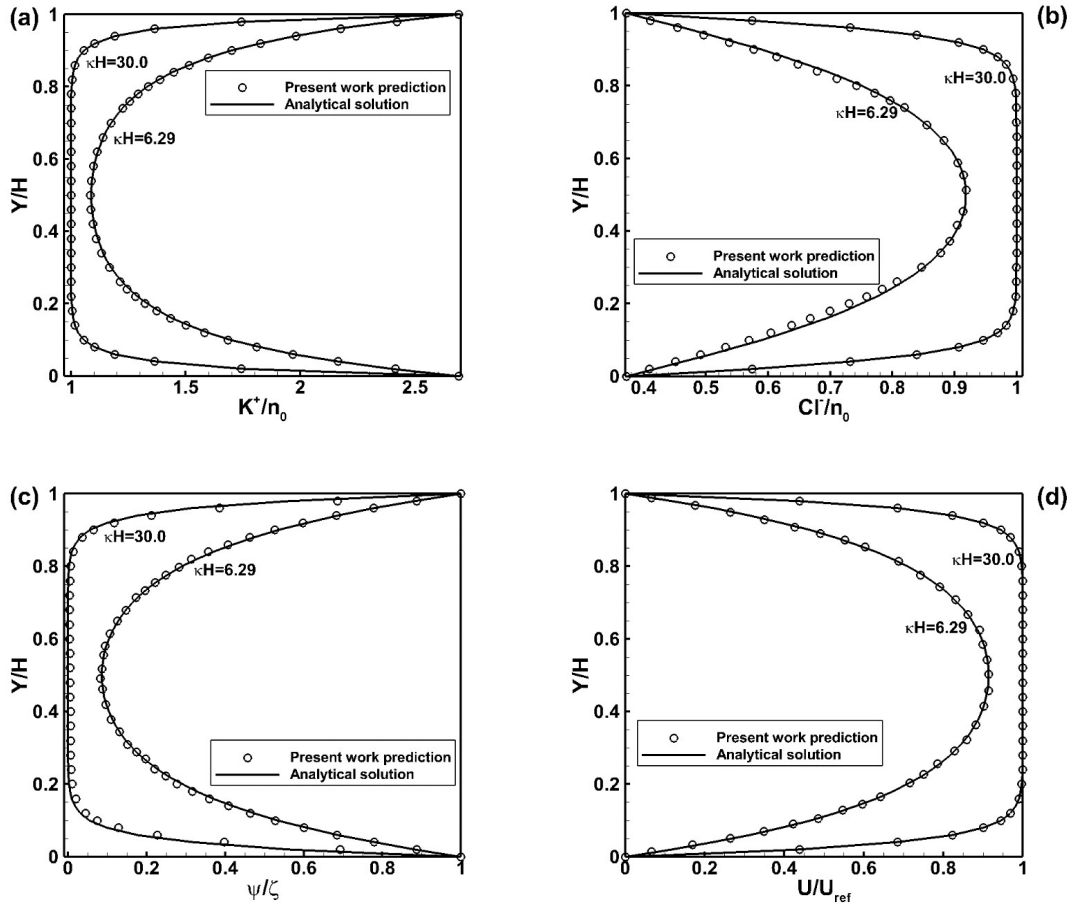

Figure 13: The dimensionless macroscopic properties (K^+, Cl^-, ψ, and U) for two EDL thickness as $\kappa H = 6.28$ and 30.0. Solid lines and circle symbols represent the analytical solution and present work local grid refinement method predictions, respectively.

relations would not be influenced by the source terms. Fig. 14 demonstrates that the FH model can not take into account the effects of the source terms in the transformation relations correctly. Consequently, one can deduce that the FH local grid refinement method could not generally applicable to model the lattice Boltzmann equations with source term.

5 Conclusions

In this contribution, we developed a general lattice Boltzmann local grid refinement algorithm for modeling the coupled multi-physics transport phenomena. By employing

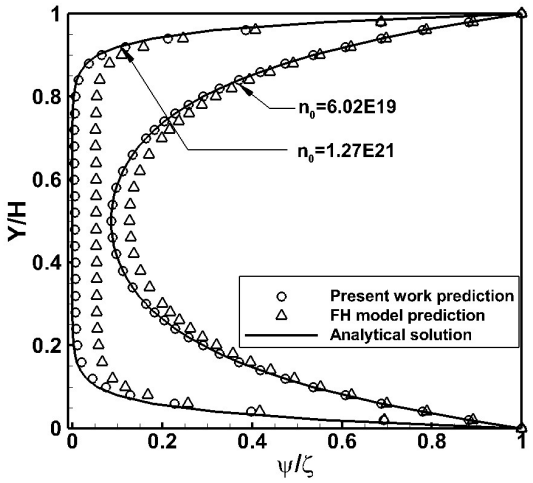

Figure 14: The dimensionless electric potential predictions by solving the Poisson-Nersnt-Planck equations for the FH and present work local grid refinement models. The velocity for the NP equation is prescribed as input parameter and equal to $\mathbf{U}=0.0$.

the Chapman-Enskog expansion, we incorporated the source term to the transformation relations of the distribution functions which interchange between fine and coarse grids. Using the proposed local grid refinement lattice Boltzmann model for momentum equations, a body-force driven Poiseuille flow was studied with four different patches (size and location). For all fine grid patches, our model could provide good predictions for velocity along the width of the channel. To examine the capability of our model for diffusion transport phenomena with uniform or variable source terms, the diffusion equation with source term was investigated for: (1) a 1D (symmetric and asymmetric) and 2D heat conduction with constant heat generation in a flat plate; (2) the electric potential distribution near to a charged wall which the source term is spatially variable and depends on the diffused property. Modeling results indicated that present work model could provide good agreement compared with the analytical solutions. Moreover, as a main application of the proposed local grid refinement algorithms for such coupled transport phenomena with source terms, the electro-osmotic flow (Poisson-Nernst-Planck with Navier-Stokes) in a microchannel was studied with two fine grid patches adjacent to the walls. The present work model can provide good agreements with the analytical solution for the flow field, ion concentration, and electric potential. To demonstrate the necessity of employing the new local grid refinement method for equations with source term, a study on the applicability of the FH model for Poisson-Nernst-Planck equations showed that the FH model could not provide correct results for electric potential. As a main conclusion, the transformation relations for fine and coarse grids in a local grid refinement method depend on the source terms in the discretized Boltzmann equation. The present local grid refinement lattice Boltzmann model provides an efficient way to model the coupled

multi-physicochemical transport phenomena in different size geometries.

Acknowledgements

This work is financially supported by the NSF grant of China (Nos. 91634107, 51676107).

References

[1] H. DAIGUJI, P. D. YANG AND A. MAJUMDAR, *Ion transport in nanofluidic channels,* Nano Lett., 4 (2004), pp. 137–142.
[2] R. B. SCHOCH, J. Y. HAN AND P. RENAUD, *Transport phenomena in nanofluidics,* Rev. Modern Phys., 80 (2008), pp. 839–883.
[3] M. TAGHIPOOR, A. BERTSCH AND P. RENAUD, *Temperature sensitivity of nanochannel electrical conductance,* ACS Nano, 9 (2015), pp. 4563–4571.
[4] T. LEI, X. MENG AND Z. GUO, *Pore-scale study on reactive mixing of miscible solutions with viscous fingering in porous media,* Comput. Fluids, 155 (2017), pp. 146–160.
[5] Y. Q. ZU AND S. HE, *Phase-field-based lattice Boltzmann model for incompressible binary fluid systems with density and viscosity contrasts*, Phys. Rev. E, 87 (2013), 043301.
[6] F.-J. YAO, K. LUO, H.-L. YI AND M. XIE, *Analysis of melting with natural convection and volumetric radiation using lattice Boltzmann method,* Int. J. Heat Mass Transfer, 112 (2017), pp. 413–426.
[7] K. LUO, J. WU, H.-L. YI AND H.-P. TAN, *Lattice Boltzmann modelling of electro-thermo-convection in a planar layer of dielectric liquid subjected to unipolar injection and thermal gradient,* Int. J. Heat Mass Transfer, 103 (2016), pp. 832–846.
[8] M. WANG AND Q. KANG, *Modeling electrokinetic flows in microchannels using coupled lattice Boltzmann methods,* J. Comput. Phys., 229 (2010), pp. 728–744.
[9] A. ALIZADEH, L. ZHANG AND M. WANG, *Mixing enhancement of low-Reynolds electro-osmotic flows in microchannels with temperature-patterned walls,* J. Colloid Interface Sci., 431 (2014), pp. 50–63.
[10] M. WANG AND Q. KANG, *Electrochemomechanical energy conversion efficiency in silica nanochannels,* Microfluid. Nanofluid., 9 (2010), pp. 181–190.
[11] M. S. HOSSAIN, X. B. CHEN AND D. J. BERGSTROM, *Fluid flow and mass transfer over circular strands using the lattice Boltzmann method,* Heat Mass Transfer, 51 (2015), pp. 1493–1504.
[12] Y. WANG, L. M. YANG AND C. SHU, *From lattice Boltzmann method to lattice Boltzmann flux solver,* Entropy, 17 (2015), pp. 7713–7735.
[13] X. X. GUO, J. K. YAO, C. W. ZHONG AND J. CAO, *A hybrid adaptive-gridding immersed-boundary lattice Boltzmann method for viscous flow simulations,* Appl. Math. Comput., 267 (2015), pp. 529–553.
[14] R. Z. HUANG AND H. Y. WU, *Total enthalpy-based lattice Boltzmann method with adaptive mesh refinement for solid-liquid phase change,* J. Comput. Phys., 315 (2016), pp. 65–83.
[15] H. Z. YUAN, Y. WANG AND C. SHU, *An adaptive mesh refinement-multiphase lattice Boltzmann flux solver for simulation of complex binary fluid flows,* Phys. Fluids, 29 (2017), 123604.
[16] J. Y. SHAO, C. SHU, J. WU AND Y. T. CHEW, *A stencil adaptive phase-field lattice Boltzmann method for two dimensional incompressible multiphase flows,* Int. J. Numer. Methods Fluids, 72 (2013), pp. 671–696.

[17] J. WU AND C. SHU, *A solution-adaptive lattice Boltzmann method for two-dimensional incompressible viscous flows,* J. Comput. Phys., 230 (2011), pp. 2246–2269.
[18] C. SHU AND Y. L. WU, *Adaptive mesh refinement-enhanced local DFD method and its application to solve NavierStokes equations,* Int. J. Numer. Methods in Fluids, 51 (2006), pp. 897–912.
[19] L. DING, C. SHU, H. DING AND N. ZHAO, *Stencil adaptive diffuse interface method for simulation of two-dimensional incompressible multiphase flows,* Comput. Fluids, 39 (2010), pp. 936–944.
[20] O. FILIPPOVA AND D. HANEL, *Acceleration of lattice-BGK schemes with grid refinement,* J. Comput. Phys., 165 (2000), pp. 407–427.
[21] O. FILIPPOVA AND D. HANEL, *Grid refinement for lattice-BGK models,* J. Comput. Phys., 147 (1998), pp. 219–228.
[22] A. FAKHARI AND T. LEE, *Finite-difference lattice Boltzmann method with a block-structured adaptive-mesh-refinement technique,* Phys. Rev. E, 89 (2014).
[23] E. BAYRAKTAR, O. MIERKA AND S. TUREK, *Benchmark computations of 3D laminar flow around a cylinder with CFX, OpenFOAM and FeatFlow,* Int. J. Comput. Sci. Eng., 7 (2012), pp. 253–266.
[24] C. L. LIN AND Y. G. LAI, *Lattice Boltzmann method on composite grids,* Phys. Rev. E, 62 (2000), pp. 2219–2225.
[25] A. DUPUIS AND B. CHOPARD, *Theory and applications of an alternative lattice Boltzmann grid refinement algorithm,* Phys. Rev. E, 67 (2003).
[26] M. ROHDE, J. J. DERKSEN AND H. E. A. VAN DEN AKKER, *An applicability study of advanced lattice-Boltzmann techniques for moving, no-slip boundaries and local grid refinement,* Comput. Fluids, 37 (2008), pp. 1238–1252.
[27] D. LAGRAVA, O. MALASPINAS, J. LATT AND B. CHOPARD, *Advances in multi-domain lattice Boltzmann grid refinement,* J. Comput. Phys., 231 (2012), pp. 4808–4822.
[28] G. EITEL-AMOR, M. MEINKE AND W. SCHROEDER, *A lattice-Boltzmann method with hierarchically refined meshes,* Comput. Fluids, 75 (2013), pp. 127–139.
[29] H. LIU, J. G. ZHOU, M. LI AND Y. ZHAO, *Multi-block lattice Boltzmann simulations of solute transport in shallow water flows,* Adv. Water Res., 58 (2013), pp. 24–40.
[30] M. STIEBLER, J. TÖLKE AND M. KRAFCZYK, *Advectiondiffusion lattice Boltzmann scheme for hierarchical grids,* Comput. Math. Appl., 55 (2008), pp. 1576–1584.
[31] I. GINZBURG, *Equilibrium-type and link-type lattice Boltzmann models for generic advection and anisotropic-dispersion equation,* Adv. Water Res., 28 (2005), pp. 1171–1195.
[32] J. K. WANG, M. WANG AND Z. X. LI, *A lattice Boltzmann algorithm for fluid-solid conjugate heat transfer,* Int. J. Therm. Sci., 46 (2007), pp. 228–234.
[33] M. R. WANG AND N. PAN, *Elastic property of multiphase composites with random microstructures,* J. Comput. Phys., 228 (2009), pp. 5978–5988.
[34] E. V. DYDEK, B. ZALTZMAN, I. RUBINSTEIN, D. S. DENG, A. MANI AND M. Z. BAZANT, *Overlimiting current in a microchannel,* Phys. Rev. Lett., 107 (2011), pp. 5.
[35] V. V. NIKONENKO, A. V. KOVALENKO, M. K. URTENOV, N. D. PISMENSKAYA, J. HAN, P. SISTAT AND G. POURCELLY, *Desalination at overlimiting currents: State-of-the-art and perspectives,* Desalination, 342 (2014), pp. 85–106.
[36] D. S. DENG, E. V. DYDEK, J. H. HAN, S. SCHLUMPBERGER, A. MANI, B. ZALTZMAN AND M. Z. BAZANT, *Overlimiting current and shock electrodialysis in porous media,* Langmuir, 29 (2013), pp. 16167–16177.
[37] M. SCHNHERR, K. KUCHER, M. GEIER, M. STIEBLER, S. FREUDIGER AND M. KRAFCZYK, *Multi-thread implementations of the lattice Boltzmann method on non-uniform grids for CPUs and GPUs,* Comput. Math. Appl., 61 (2011), pp. 3730–3743.
[38] J. TÖLKE, S. FREUDIGER AND M. KRAFCZYK, *An adaptive scheme using hierarchical grids for*

lattice Boltzmann multi-phase flow simulations, Comput. Fluids, 35 (2006), pp. 820–830.
[39] D. YU, R. MEI AND W. SHYY, *A multi-block lattice Boltzmann method for viscous fluid flows,* Int. J. Numer. Methods Fluids, 39 (2002), pp. 99–120.
[40] D. Z. YU, R. W. MEI, L. S. LUO AND W. SHYY, *Viscous flow computations with the method of lattice Boltzmann equation,* Progress Aerospace Sci., 39 (2003), pp. 329–367.
[41] P. DUTTA AND A. BESKOK, *Analytical solution of combined eloectoossmotic/pressure driven flows in two-dimensional straight channels: Finite debye layer effects,* Anal. Chem., 73 (2001), pp. 1979–1986.
[42] P. DUTTA, A. BESKOK AND T. C. WARBURTON, *Numerical simulation of mixed electroosmotic/pressure driven microflows,* Numer. Heat Transfer Part Appl., 41 (2002), pp. 131–148.
[43] S. CHEN AND G. D. DOOLEN, *Lattice Boltzmann method for fluid flows,* Annu. Rev. Fluid Mech., 30 (1998), pp. 329–364.
[44] X. HE, S. CHEN AND G. D. DOOLEN, *A novel thermal model for the lattice Boltzmann method in incompressible limit,* J. Comput. Phys., 146 (1998), pp. 282–300.
[45] H. D. CHEN, S. Y. CHEN AND W. H. MATTHAEUS, *Recovery of the navier-stokes equations using a lattice-gas boltzmann method,* Phys. Rev. A, 45 (1992), pp. R5339–R5342.
[46] M. WANG AND Q. KANG, *Modeling electrokinetic flows in microchannels using coupled lattice Boltzmann methods,* J. Comput. Phys., 229 (2010), pp. 728–744.
[47] Z. GUO, C. ZHENG AND B. SHI, *Discrete lattice effects on the forcing term in the lattice Boltzmann method,* Phys. Rev. E, 65 (2002), 046308.
[48] V. S. ARPACI, Conduction heat transfer, Pearson Custom Pub; Abridged edition, (1991).
[49] D. LI, Electrokinetics in Microfluidics, Elsevier Academic Press, (2004).
[50] M. WANG AND S. CHEN, *Electroosmosis in homogeneously charged micro- and nanoscale random porous media,* J. Colloid Interface Sci., 314 (2007), pp. 264–273.
[51] P. C. LICHTNER, *Principles and practice of reactive transport modeling,* Scientific Basis for Nuclear Waste Management XVII, Symposium, 111 (1995), pp. 117–130.
[52] J. H. MASLIYAH AND S. BHATTACHARJEE, Electrokinetic and Colloid Transport Phenomena, John Wiley & Sons, New Jersey, (2006).
[53] A. ALIZADEH AND M. WANG, *Direct simulation of electroosmosis around a spherical particle with inhomogeneously acquired surface charge,* Electrophoresis, (2016).
[54] A. ALIZADEH, M. E. WARKIANI AND M. WANG, *Manipulating electrokinetic conductance of nanofluidic channel by varying inlet pH of solution,* Microfluid. Nanofluid., 21 (2017), pp. 52.